Isothermal and Nonisothermal Crystallization Kinetics of a Semicrystalline Copolyterephthalamide Based on Poly(decamethylene terephthalamide)

Hongzhi Liu, Guisheng Yang, Aihua He, Meiyan Wu

Joint Laboratory of Polymer Science and Material, Institute of Chemistry, Chinese Academy of Science, Beijing 100080, China

Received 28 September 2003; accepted 31 May 2004
DOI 10.1002/app.21011
Published online in Wiley InterScience (www.interscience.wiley.com).

ABSTRACT: The isothermal and nonisothermal crystallization kinetics of a semicrystalline copolyterephthalamide based on poly(decamethylene terephthalamide) (PA-10T) was studied by differential scanning calorimetry. Several kinetic analyses were used to describe the crystallization process. The commonly used Avrami equation and the one modified by Jeziorny were used, respectively, to describe the primary stage of isothermal and nonisothermal crystallization. The Avrami exponent n was evaluated to be in the range of 2.36–2.67 for isothermal crystallization, and of 3.05–5.34 for nonisothermal crystallization. The Ozawa analysis failed to describe the nonisothermal crystallization behavior, whereas the Mo–Liu equation, a combination equation of Avrami and Ozawa formulas, successfully described the nonisothermal crystallization kinetics. In addition, the value of crystallization rate coefficient under nonisothermal crystallization conditions was calculated. © 2004 Wiley Periodicals, Inc. J Appl Polym Sci 94: 819–826, 2004

Key words: polyamides; crystallization; kinetics (polym.); differential scanning calorimetry (DSC); melting point

INTRODUCTION

Polyterephthalamides (PTPAs) are partially aromatic polyamides consisting of terephthalic acid and aliphatic diamine monomer units. To lower melting points and to improve their processability, additional monomers, such as isophthalic acid,[1] adipic diacid,[2] and ε-caprolactam,[3] may be included as comonomers [e.g., poly(hexamethylene terephthalamide) (PA-6T)]. The resultant PTPAs may be either amorphous or semicrystalline, depending on their composition.[4] Compared with common aliphatic polyamides such as nylon-6 and nylon-66, semicrystalline PTPAs are generally characterized by higher melting points; higher glass-transition temperatures; better chemical resistance; and lower moisture absorption, thus having better dimensional stability under moist conditions. Therefore PTPAs are particularly suitable for uses in electronics, engineering plastics, and fibers.

Until now, commercially available PPTAs are mainly based on PA-6T. In consideration of improving flexibility of macromolecules backbones, which may change the crystallization behavior and other properties of PPTAs, longer-chain aliphatic diamines were used instead of hexamethylene diamine in PA-6T. For example, PPTAs based on poly(nonamethylene terephthalamide) (PA-9T) using nonamethylene diamine, poly(decamethylene terephthalamide) (PA-10T) using decamethylene diamine, and poly(dodecamethylene terephthalamide) (PA-12T) using dodecamethylene diamine as raw materials were previously synthesized and reported in the literature.[5–10] We are particularly interested in the PPTAs based on PA-10T. This is because of the ample resource of decamethylene diamine in China, which was synthesized from the natural product castor oil.

Despite finding several studies that dealt with the synthesis of semicrystalline PA-10T[5–7] during a review of the literature, there are few reports about its physical properties.

It is well known that the crystallization process dramatically affects polymer properties through the crystal structure and morphology established during the solidification process. As an important aspect of the crystallization process, the study of polymer crystallization kinetics is significant both from the theoretical and the practical perspective. Additionally, to reach the optimum condition in an industrial process and to obtain products with better properties, it is necessary to estimate the rate of crystallization in the nonisothermal process. Equally important from both the scientific and the product development perspectives, it is also necessary to compare the relative crystallization rates of different polymer systems.

Correspondence to: G. Yang (ygs@geniuscn.com).

In this article, the isothermal and nonisothermal crystallization kinetics of the aforementioned semicrystalline copolyterephthalamide, based on PA-10T, were investigated by differential scanning calorimetry. Several kinetics methods were applied to analyze its crystallization process. Besides, a method to evaluate the nonisothermal crystallization rate with a crystallization rate coefficient (CRC) parameter, proposed by Khanna, was used to compare the semicrystalline PA-10T with other common aliphatic polyamides (e.g., PA-6 and -66).

EXPERIMENTAL

Materials and preparation

The additive-free semicrystalline copolyterephthalamide used for this study, based on PA-10T, was kindly provided by Shanghai Genius Advanced Materials Co., Ltd (China) in the form of pellets. It is a random copolymer that was synthesized by melt polycondensation of the decamethylene diamine salt of terephthalic acid, the decamethylene diamine salt of isophthalic acid, and ε-caprolactam, which are designated 10T, 10I, and CAP, respectively. The chemical structures of its repeating units are presented as follows:

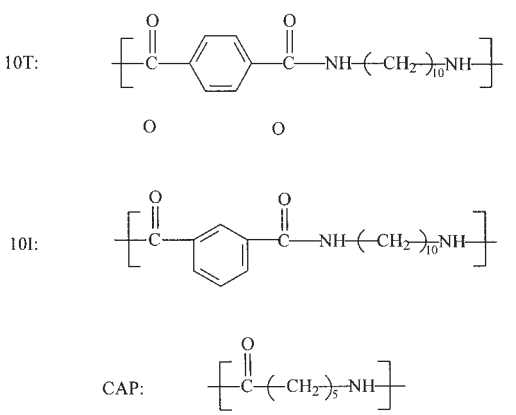

where the molar ratio of the three repeating units 10T : 10I : CAP = 8 : 1 : 1.

Synthesis procedures were as follows: to a 5-L autoclave were charged the required amounts of 10T salt, 10I salt, and caprolactam. The mixture were slowly heated under a nitrogen atmosphere while the pressure was increased to 2 MPa and then kept constant. As the temperature was elevated to 310°C, the pressure began to level off. Finally, when the temperature reached 330°C, the reaction was further carried out at atmospheric pressure for 0.5–1 h and the resulting polymer, designated as SCPA-10T, had an intrinsic viscosity of 0.72, as measured in concentrated sulfuric acid (98%) at 25°C. The sample was dried under vacuum at 80°C for 12 h before measurements.

Differential scanning calorimetry

Isothermal and nonisothermal crystallization kinetics were studied using a Perkin–Elmer DSC-7 differential scanning calorimeter (Perkin Elmer Cetus Instruments, Norwalk, CT), where the temperature was calibrated with an indium standard. All DSC measurements were performed under a nitrogen atmosphere, and sample weights varied from 6 to 8 mg.

Isothermal and nonisothermal crystallization processes

For isothermal crystallization kinetic studies, the samples were first heated to 350°C and maintained at this temperature for 3 min to erase thermal history, and then samples were quenched at 200°C/min to the five designated crystallization temperatures (T_c = 283, 284, 285, 286, 287°C, respectively). The exothermic curves, as a function of time, were then recorded and investigated. After erasing the previous thermal history, nonisothermal crystallization kinetics was performed by the cooling of the melts at five different cooling rates (5, 10, 20, 30, 40°C/min, respectively). The exothermic curves of heat flow, as a function of temperature, were recorded and investigated.

RESULTS AND DISCUSSION

Isothermal crystallization kinetics: Avrami equation

The SCPA-10T obtained is semicrystalline, which is opaque in appearance. Its melting temperature (T_m) and glass-transition temperature (T_g) are 305.8 and 109.1°C, respectively.

Because the crystallization rate of SCPA-10T is very fast, the range of isothermal crystallization temperature for the kinetic study is limited to 283–287°C. Figure 1 shows the exothermic traces for the melt crystallization of semicrystalline PA-10T at various isothermal crystallization temperatures. It can be seen clearly from Figure 1 that the crystallization exothermic peak shifts to a longer time and becomes flat with increasing crystallization temperature T_c, which implies that the sample with higher crystallization temperature requires a longer time to complete crystallization. In the study, the relative degree of crystallinity at time t, $X(t)$, was calculated according to the following equation:

$$X(t) = \frac{\int_0^t \frac{dH}{dt} dt}{\int_0^\infty \frac{dH}{dt} dt} = \frac{\Delta H_t}{\Delta H_\infty} \quad (1)$$

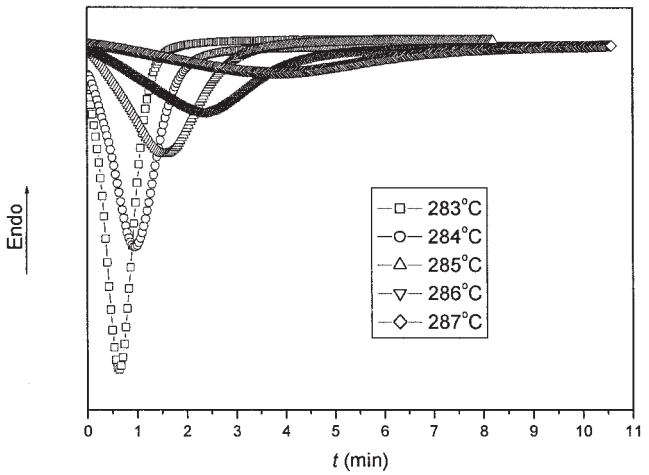

Figure 1 Plots of heat flow versus time t for the isothermal crystallization of SCPA-10T at different crystallization temperatures by DSC.

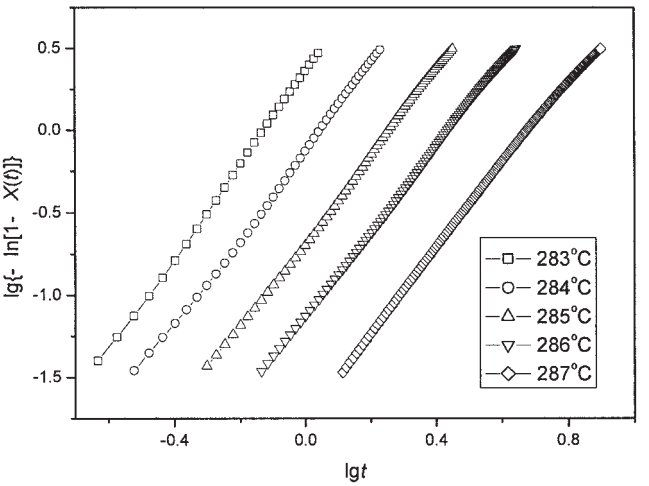

Figure 2 Plots of $\log\{-\ln[1 - X(t)]\}$ versus $\log t$ for the isothermal crystallization of SCPA-10T at different crystallization temperatures.

where dH/dt is the rate of heat evolution; ΔH_t is the heat generated at time t; and ΔH_∞ is the total heat generated up to the end of the crystallization process.

In general, the process of isothermal crystallization is composed of two stages: the primary crystallization stage and the secondary crystallization stage. The whole crystallization process is markedly temperature dependent. Assuming that the relative degree of crystallinity increases with increasing crystallization time t, then the Avrami equation [eq. (1)[rsqb][11,12] can be used to analyze the isothermal melt-crystallization process of SCPA-10T, as follows:

$$X(t) = 1 - \exp(-Kt^n)$$

$$\log\{-\ln[1 - X(t)]\} = n\log t + \log K \quad (2)$$

where n is the Avrami exponent dependent on the mechanism of nucleation and on the form of crystal growth, and K is the isothermal crystallization rate parameter. In general, the values of n should be an integer between 1 and 4 for different crystallization mechanisms. However, the Avrami exponent is not a straightforward integer, and other complex factors are probably involved during the process.

The plots of $\log\{-\ln[1 - X(t)]\}$ versus $\log t$ are shown in Figure 2. Each curve shows an initial linear portion, then subsequently tends to level off. The deviation becomes more obvious with decreasing T_c. This deviation is probably attributable to the secondary crystallization, which is caused by the spherulite impingement in the later stage of the crystallization process.[13,14]

From the slope and intercept of the initial linear portion in Figure 2, the values of n and K were determined and are listed in Table I. The obtained Avrami exponent n varies from 2.36 to 2.67, depending on the crystallization temperature T_c. These results indicate that the crystal in the initial stage grows in two dimensions, controlled by thermal nucleation. The values of the crystallization rate parameters K increase with decreasing crystallization temperature T_c (Table I), which indicates that SCPA-10T exhibits a very different temperature dependency, characteristic of nucleation-controlled and thermal-activated crystallization associated with the proximity of the melting temperature T_m.

Figure 3 shows the plots of $X(t)$ versus crystallization time t for SCPA-10T at different crystallization temperatures. It can be seen that characteristic sigmoidal isotherms are shifted to the right with increasing isothermal crystallization temperatures, indicating that the crystallization rate becomes slower.

Another important parameter is the half-time of crystalization $t_{1/2}$, which is defined as the time taken from the onset of the crystallization until 50% completion and can be determined from the measured kinetics parameters. That is,

TABLE I
Kinetic Parameters for the Isothermal Crystallization of SCPA-10T

	T_c (°C)				
Parameter	283	284	285	286	287
n	2.57	2.36	2.43	2.48	2.67
K, min^{-n}	1.66	0.59	0.20	0.07	0.02
t_{max}, min	0.68	0.99	1.56	2.37	3.63
$t_{1/2}$, min	0.71	1.07	1.67	2.52	3.77
$T_{1/2}$, min^{-1}	1.41	0.93	0.60	0.40	0.27
$X(t_{max})$, %	46.56	49.11	48.99	49.10	43.47

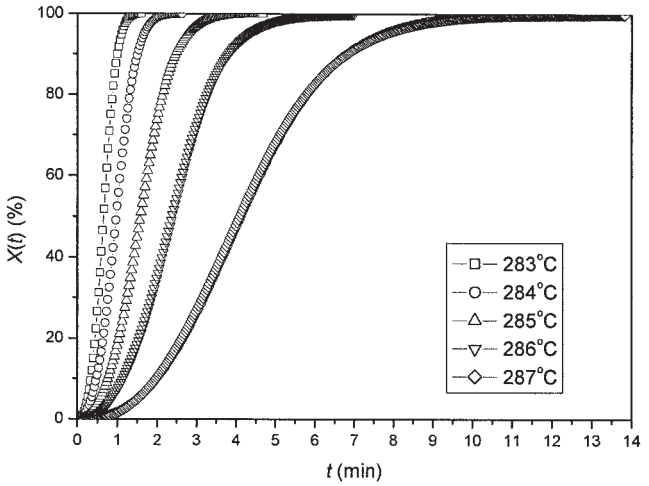

Figure 3 Development of the relative degree of crystallinity $X(t)$ with crystallization times t for the isothermal crystallization of SCPA-10T at different crystallization temperatures.

$$t_{1/2} = \left(\frac{\ln 2}{K}\right)^{1/n} \tag{3}$$

The dependency of $t_{1/2}$ on the crystallization temperature is shown in Figure 4. As observed in all polymeric materials, $t_{1/2}$ increases slowly with increasing T_c, indicating that the rate of crystallization is faster when the degree of supercooling is greater.

Usually, the crystallization rate (G) is described as the reciprocal of $t_{1/2}$ [e.g., $G = \tau_{1/2} = (t_{1/2})^{-1}$]. The values of $\tau_{1/2}$, $t_{1/2}$, and $X(t_{max})$ are listed in Table I. Lin[15] used eq. (2) to calculate the necessary time for maximum crystallization rate t_{max} because this time corresponds to the point at which $dQ(t)/dt = 0$, where $Q(t)$ is the heat-flow rate, obtaining

$$t_{max} = \left(\frac{n-1}{nK}\right)^{1/n} \tag{4}$$

The calculated values of t_{max} are listed in Table II. Data of t_{max} can also be obtained from the heat-flow curves in Figure 1.

TABLE II
Values of T^*, t_{max}, ΔH_c, and $X(t)$ During the Nonisothermal Crystallization of SCPA-10T

	R (°C/min)				
Parameter	5	10	20	30	40
T^*, °C	279.4	276.3	270.7	266.9	263.9
t_{max}, min	1.52	0.73	0.50	0.41	0.33
ΔH_c, J/g	36.76	42.37	46.31	47.88	47.83
$X(t_{max})$, %	43.51	40.53	48.40	49.79	48.67

Nonisothermal crystallization kinetics: Jeziorny-modified Avrami equation

In practical processing, such as extrusion, injection molding, and film production, crystallization usually proceeds under dynamic nonisothermal conditions, so it is of practical significance to study the crystallization kinetics under nonisothermal conditions, particularly for the technological optimization and manufacture of high-performance polymeric materials.

The nonisothermal crystallization exothermic curves of SCPA-10T at various cooling rates (R) are shown in Figure 5. T^* is the peak temperature at which the crystallization rate was maximum, and T^* shifts to

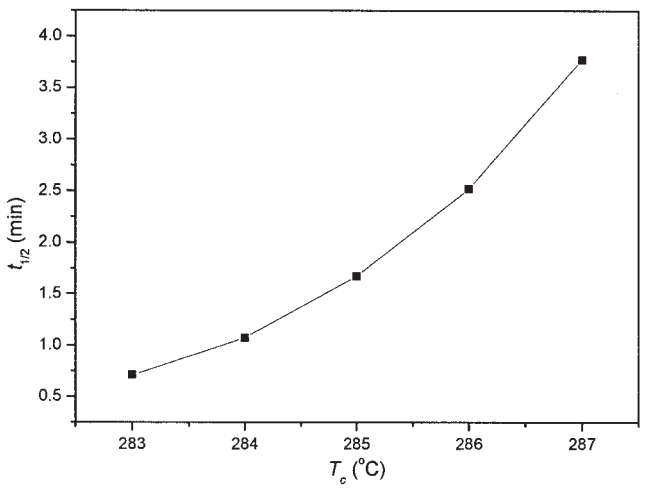

Figure 4 The plot of half-time of crystallization $t_{1/2}$ versus the crystallization temperature T_c for the isothermal crystallization of SCPA-10T.

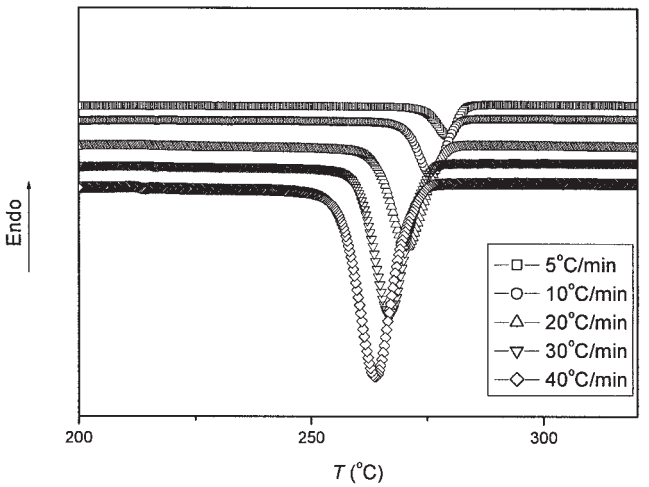

Figure 5 Plots of heat flow versus temperature T during nonisothermal crystallization of SCPA-10T at different cooling rates by DSC.

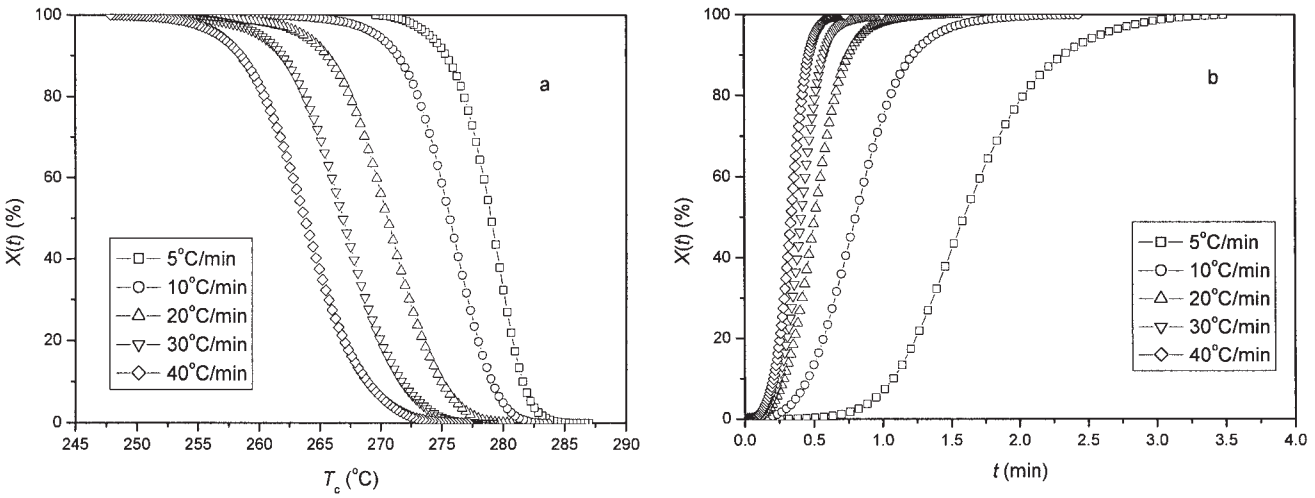

Figure 6 Development of the relative degree of crystallinity $X(t)$ with (a) crystallization temperatures T_c and (b) crystallization times t for the nonisothermal crystallization of SCPA-10T at different cooling rates.

a lower temperature region with increasing cooling rates. This observation is typical of other samples and a common phenomenon for semicrystalline polymer crystallized nonisothermally. When the polymer was undergoing crystallization at a lower cooling rate, it had a relatively long time remaining within the temperature range that promoted sufficient mobility of segments for the growth of crystallites; when cooled at a relatively rapid rate, however, segments were frozen before the formation of regular crystallite, thereby decreasing the crystallization temperature. The values of T^*, the corresponding time t_{max}, and the crystallization enthalpies at different cooling rates are listed in Table II.

From the DSC data, we can calculate the values of the relative degree of crystallinity $X(t)$ at different crystallization temperatures T_c, as shown in Figure 6(a). During the nonisothermal crystallization process, we obtained a series of reversed S-shaped curves. A relationship between T_c and time crystallization time t is given as follows:

$$t = \frac{|T_0 - T_c|}{R} \tag{5}$$

where T_0 is the initial temperature when crystallization begins ($t = 0$) and R is the cooling rate. With eq. (5), the horizontal temperature axis in Figure 6(a) can be transformed into a timescale [Fig. 6(b)]. Because of the spherulite impingement in the later stage of crystallization, the curves tend to flatten and became S-shaped (or reversed S-shaped). The higher the cooling rate, the shorter the time of crystallization completion. We can obtain the values of T_c or t at the various cooling rates from Figure 6 at a random relative degree of crystallinity $X(t)$. The values of $X(t)$ at the peak temperature T^* are also shown in Table II.

Mandelkern[16] considered that the primary stage of nonisothermal crystallization can be described by the Avrami equation, based on the assumption that the crystallization temperature (T_c) is constant. Mandelkern obtained the following equation:

$$1 - X(t) = \exp(-Z_t t^n)$$

$$\log\{-\ln[1 - X(t)]\} = n\log t + 1°\mathrm{g}Z_t \tag{6}$$

where Z_t is the rate constant in the nonisothermal crystallization process. Jeziorny considered that the values of Z_t, determined by Avrami eq. (6), should be adequate. Considered to be an influence on the cooling or heating rate $R = dT/dt$, Jeziorny[17] assumed that R was constant or approximately constant. The final form of the rate parameter characterizing the kinetics of nonisothermal crystallization is given as follows:

$$\log Z_c = \frac{\log Z_t}{R} \tag{7}$$

Drawing the straight line corresponding to $\log\{-\ln[1 - X(t)]\}$ versus $\log t$ by using eq. (6), we can determine the Avrami exponent n and the rate parameter Z_t or Z_c from the slope and intercept (Fig. 7). The values of Z_t, Z_c, and $t_{1/2}$ are shown in Table III. Apparently, the values of the Avrami exponent n from the first crystallization process are much larger than those of the secondary. Like the previous treatments for the isothermal crystallization kinetics of SCPA-10T (Fig. 2), all the curves are divided into the following two sections: the primary crystallization stage and the secondary crystallization stage. At the secondary stage, the straight line tends to deviate from the primary crystallization stage, especially at lower cooling rate. At the primary stage, the Avrami exponent, n_1 in the

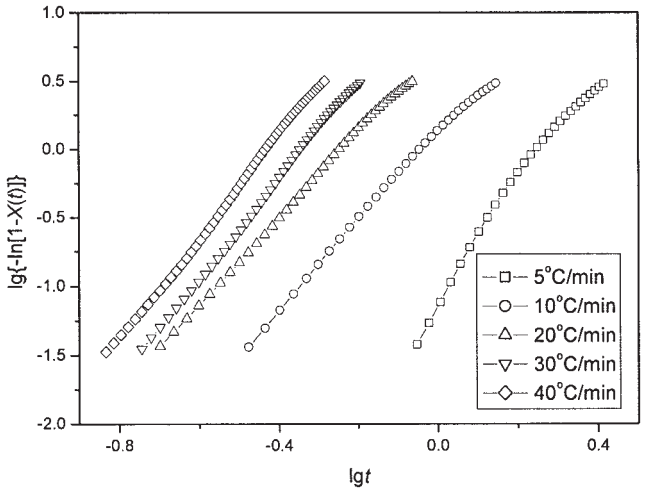

Figure 7 Plots of $\log\{-\ln[1 - X(t)]\}$ versus $\log t$ for the nonisothermal crystallization of SCPA-10T at different cooling rates.

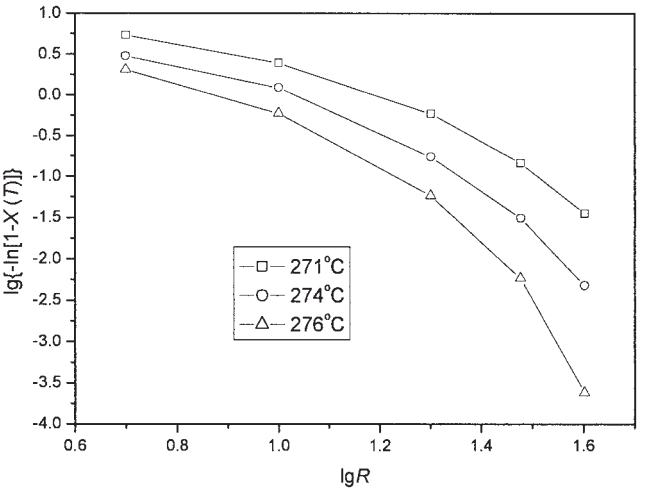

Figure 8 Plots of $\log\{-\ln[1 - X(T)]\}$ versus $\log R$ from the Ozawa equation for SCPA-10T.

range of 3.05–5.34, indicates that the mode of the nucleation and growth at primary stage of the nonisothermal crystallization for SCPA-10T is more complicated than that for the isothermal crystallization process. At the secondary stage, the Avrami exponent, n_2 = 2.17–3.04 (Table III), because of the spherulites' impingement and crowding, the mode becomes simpler.

Ozama analysis in nonisothermal crystallization kinetics

Considering the effect of the cooling rate R on dynamic crystallization by properly modifying the Avrami equation, Ozawa[18] extended the Avrami equation to the process of nonisothermal crystallization, as follows:

$$1 - X(T) = \exp\left[-\frac{K(T)}{R^m}\right]$$

$$\log\{-\ln[1 - X(T)]\} = -m\log R + \log K(T) \quad (8)$$

where $X(T)$ is the relative degree of crystallinity, m is the Ozawa exponent, and $K(T)$ is the kinetic crystallization rate constant. A plot of $\log\{-\ln[1 - X(T)]\}$ versus $\log R$ at a given temperature should result in a straight line if the Ozawa method is valid. However, we did not obtain straight lines in Figure 8. This experimental fact indicates that the Ozawa equation is not suitable to describe the kinetics in the nonisothermal crystallization process of semicrystalline PA-10T, which has an appreciable extent of secondary crystallization.

Combined Avrami equation and Ozawa equation

To find a method to describe properly the nonisothermal crystallization process, Liu and coworkers[19] proposed a novel method for nonisothermal crystallization process and successfully dealt with the nonisothermal crystallization behavior of nylon-11,[20] PEDEKK,[21] nylon-66,[22] nylon-46,[23] nylon-1212,[24] syndiotactic polystyrene,[25] PP–PP-*g*-MAH–Org–MMT,[26] and PETIS.[27] They obtained the following equations by relating eq. (6) to eq. (8):

TABLE III
Values of n, Z_t, Z_c, and $\tau_{1/2}$ from the Avrami Equation at the Two Stages of Nonisothermal Crystallization for SCPA-10T

	Primary crystallization stage				Secondary crystallization stage			
R (°C/min)	n_1	Z_{t1}	Z_{c_1}	$\tau_{1/2}$ (min^{-1})	n_2	Z_{t2}	Z_{c2}	$T_{1/2}$ (min^{-1})
5	5.34	0.072	0.59	0.97	2.46	0.29	0.78	1.05
10	3.40	1.52	1.04	1.13	2.18	1.48	1.04	1.20
20	3.05	4.95	1.08	1.16	2.35	4.46	1.08	1.21
30	3.40	11.92	1.09	1.14	2.86	11.14	1.08	1.17
40	3.37	21.10	1.08	1.14	3.04	23.26	1.08	1.16

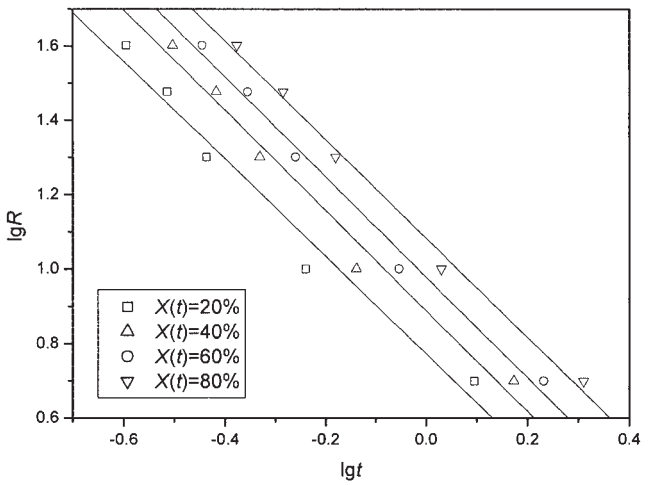

Figure 9 Plots of log R versus log t from the combined Avrami and Ozawa equation for SCPA-10T.

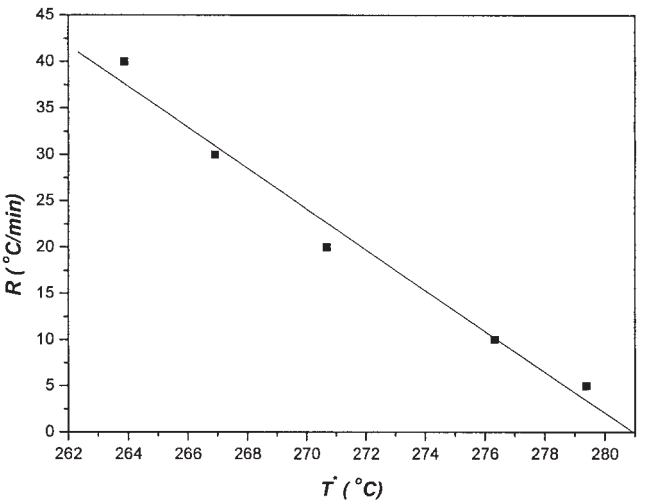

Figure 10 Dependency of the melt-crystallization peak temperature (T^*) on the cooling rate (R) for SCPA-10T during the nonisothermal crystallization process.

$$\log Z_t + n\log t = \log K(T) - m\log R$$

$$\log R = \frac{1}{m}\log\left[\frac{K(T)}{Z_t}\right] - \frac{n}{m}\log t \quad (9)$$

Define $F(T) = [K(T)/Z_t]^{1/m}$ and $\alpha = n/m$. The parameter $F(T)$ is the value of the cooling rate, which has to be chosen at the unit crystallization time when the measured system amounts to a certain degree of crystallinity. The smaller the value of $F(T)$, the higher the crystallization rate becomes. Therefore, $F(T)$ had a definite physical and practical meaning. By the above assumption, Liu and coworkers obtained the following expression:

$$\log R = \log F(T) - \alpha\log t \quad (10)$$

At a given relative degree of crystallinity, the plots of log R versus log t, according to eq. (10), are shown in Figure 9. Using straight lines to fit these data points, we can obtain a series of lines with slope $= -\alpha$ and intercept = log $F(T)$. The values of α and $F(T)$ are listed in Table IV. It is apparent that the values of $F(T)$ systematically increase with increasing relative degree of crystallinity, indicating that at unit crystallization time, a higher cooling rate should be used to obtain a higher degree of crystallinity; however, the values of α are approximately constant.

TABLE IV
Values of α and $F(T)$ at a Certain Relative Degree of Crystallinity $X(t)$ from Equation (10) of SCPA-10T

	$X(t)$ (%)			
Variable	20	40	60	80
α	1.31	1.35	1.35	1.33
$F(T)$	5.92	7.73	9.51	12.10

Crystallization rate coefficient

To allow a direct comparison of the crystallization rates of various polymers on a single scale, empirical methods were proposed.[28–30] Among them, Khanna[28] introduced a "crystallization rate coefficient" (CRC), defined as the variation in cooling rate, required to change the supercooling of the polymer melt, of 1°C. The CRC can be measured from the slope of the plot of cooling rate versus crystallization peak temperature and can be used as a guide for ranking the polymers on a scale of crystallization rates. The CRC values are higher for faster crystallization systems. At the same time, Khanna presented a series of CRC values for different polymers.

According to Khanna's treatment, the cooling rate R is plotted against T^*, as shown in Figure 10, and the CRC value of SCPA-10T obtained from the slope of the line is 132.2 h^{-1}. Compared with the values reported for other aliphatic polyamides such as PA-6, -66, and -46, the CRC of SCPA-10T is appreciably higher (values of CRC for PA-6, -66, and -46 are 79.6, 82.4, and 81.5 h^{-1}, respectively), which is beneficial for injection-molded fabrication resulting from reduction in cycle time.

CONCLUSION

The study of bulk crystallization kinetics of polymers is an important step in understanding, predicting, and designing structural formation under various processing conditions. In this article, the isothermal and

nonisothermal crystallization kinetics of SCPA-10T were investigated by DSC. The Avrami analysis indicates that the crystallization process is composed of the primary stage and the secondary stage. At the primary stage of the isothermal crystallization process, the Avrami exponent n varies from 2.36 to 2.67, indicating that crystal growth is in two-dimensional extensions during the primary stage.

For the nonisothermal crystallization process, several different analytical methods were explored to investigate the nonisothermal crystallization behavior. The Avrami equation modified by Jeziorny was used to describe the primary stage of nonisothermal crystallization with the exponent n_1 in the range of 3.05–5.34, indicating that the mode of spherulitic nucleation and growth is more complicated than that in the isothermal crystallization process. At the secondary stage, however, the crystallization time is lengthened, the spherulites are impinged and crowded, the crystallization rate decreases, and the mode of spherulitic nucleation and growth becomes simple (n_2 = 2.17–3.04). The Ozawa equation failed to describe the nonisothermal crystallization process, although with Mo's method, the nonisothermal crystallization process of SCPA-10T was successfully analyzed. Based on Khanna's method, the calculated CRC value for SCPA-10T is 132.2 h^{-1}, which suggests that SCPA-10T has a high crystallization rate relative to that of the common aliphatic polyamide.

References

1. Bier, G.; Blaschke, F.; Der Funten, H. A.; Schade, G. U.S. Pat. 4,111,921, 1978.
2. Edgar, O. B.; Hill, R. J Polym Sci 1952, 8, 1.
3. Ajroldi, G.; Stea, G.; Mattiussi, A.; Fomagalli, M. J Appl Polym Sci 1973, 17, 3185.
4. Dolden, J. G. Polymer 1976, 17, 875.
5. Davis, A. C.; Edwards, T. E. Brit. Pat. 1070416, 1967.
6. Liedloff, H. J.; Schmid, M. U.S. Pat. 5,708,125, 1998.
7. Ng, H. U.S. Pat. 6,355,769, 2002.
8. Keen, W. E.; Kirkaldy, D. U.S. Pat. 3,642,710, 1972.
9. Chapman, R. D.; Pichett, O. A. U.S. Pat. 3,917,561, 1975.
10. Saotome, K.; Komoto, H.; J Polym Sci Part A-1 1966, 4, 1463.
11. Avrami, M. J Chem Phys 1939, 7, 1103.
12. Avrami, M. J Chem Phys 1940, 8, 212.
13. Wunderlich, B. Macromolecular Physics, Vol. 2; Academic Press: New York, 1977.
14. Liu, J. P.; Mo, Z. S. Chin Polym Bull 1991, 4, 199.
15. Lin, C. C. Polym Eng Sci 1983, 23, 113.
16. Fava, R. A. Methods of Experimental Physics; Academic Press: New York, 1980; Vol. 16, Part B.
17. Jeziorny, A. Polymer 1978, 19, 1142.
18. Ozawa, T. Polymer 1971, 12, 150.
19. Liu, T. X.; Mo, Z. S.; Feng, Z. L. Polym Eng Sci 1997, 37, 568.
20. Liu, S. Y.; Yu, Y. N.; Cui, Y.; Zhang, H. F.; Mo, Z. S. J Appl Polym Sci 1998, 70, 2371.
21. Liu, T. X.; Mo, Z. S.; Zhang, H. F. J Polym Eng 1998, 18, 283.
22. Zhang, Q. X; Mo, Z. S. Chin J Polym Sci 2001, 19, 237.
23. Zhang, Q. X.; Zhang, Z. H.; Zhang, H. F.; Mo, Z. S. J Polym Sci Part B: Polym Phys 2002, 40, 1784.
24. Liu, M. Y.; Zhao, Q. X.; Wang, Y. D.; Zhang, C. G.; Mo, Z. S.; Cao, S. K. Polymer 2003, 44, 2537.
25. Chen, Q. Y.; Yu, Y. N.; Na, T. N.; Zhang, H. F.; Mo, Z. S. J Appl Polym Sci 2002, 83, 2528.
26. Xu, W. B.; Liang, G. D.; Wang, W.; Tang, S. P.; He, P. S.; Pan, W. B. J Appl Polym Sci 2003, 88, 3093.
27. Xiao, J.; Zhang, H. L.; Wan, X. H.; Zhang, D.; Zhou, Q. F.; Woo, E. M.; Turner, S. R. Polymer 2002, 43, 3683.
28. Khanna, Y. P. Polym Eng Sci 1990, 30, 1615.
29. Roerdink, E.; Warnier, J. M. M. Polymer 1985, 26, 1582.
30. Zhang, R. Y.; Zheng, H. F.; Lou, X. L.; Ma, D. Z. J Appl Polym Sci 1994, 51, 51.